Proc. Natl. Acad. Sci. USA
Vol. 90, pp. 5767–5771, June 1993
Biophysics

Relaxation kinetics of the Na^+/glucose cotransporter

(Na⁺/glucose symporter/pre-steady-state current/charge movement)

DONALD D. F. LOO, AKIHIRO HAZAMA, STÉPHANE SUPPLISSON, ERIC TURK, AND ERNEST M. WRIGHT

Department of Physiology, University of California, Los Angeles, School of Medicine, Los Angeles, CA 90024-1751

Communicated by Jared M. Diamond, March 22, 1993

ABSTRACT **An important class of integral membrane proteins, cotransporters, couple solute transport to electrochemical potential gradients; e.g., the Na^+/glucose cotransporter uses the Na^+ electrochemical potential gradient to accumulate sugar in cells. So far, kinetic analysis of cotransporters has mostly been limited to steady-state parameters. In this study, we have examined pre-steady-state kinetics of Na^+/glucose cotransport. The cloned human transporter (hSGLT1) was expressed in *Xenopus* oocytes, and voltage-clamp techniques were used to monitor current transients after step changes in membrane potential. Transients exhibited a voltage-dependent time constant (τ) ranging between 2 and 10 ms. The charge movement Q was fitted to a Boltzmann relation with maximal charge Q_{max} of ≈20 nC, apparent valence z of 1, and potential $V_{0.5}$ of −39 mV for 50% Q_{max}. Lowering external Na^+ from 100 to 10 mM reduced Q_{max} 40%, shifted $V_{0.5}$ from −39 to −70 mV, had no effect on z, and reduced the voltage dependence of τ. Q_{max} was independent of, but τ was dependent on, temperature (a 10°C increase increased τ by a factor of ≈2.5 at −50 mV). Addition of sugar or phlorizin reduced Q_{max}. Analyses of hSGLT1 pre-steady-state kinetics indicate that charge transfer upon a step of membrane potential in the absence of sugar is due to two steps in the reaction cycle: Na^+ binding/dissociation (30%) and reorientation of the protein in the membrane field (70%). The rate-limiting step appears to be Na^+ binding/dissociation. Q_{max} provides a measure of transporter density (≈$10^4/\mu m^2$). Charge transfer measurements give insight into the partial reactions of the Na^+/glucose cotransporter, and, combined with genetic engineering of the protein, provide a powerful tool for studying transport mechanisms.**

Cotransporters are membrane transport proteins widely expressed in bacterial, plant, and animal cells (1, 2) which couple the transport of sugars, amino acids, neurotransmitters, osmolytes, and ions into cells to electrochemical potential gradients (Na^+, H^+, Cl^-). An important example is the Na^+/glucose cotransporter, which is responsible for the "active" accumulation of sugars in epithelial cells of the intestine.

In recent electrophysiological experiments designed to measure steady-state kinetic properties of the cloned Na^+/glucose cotransporter (SGLT1) expressed in *Xenopus* oocytes we observed pre-steady-state currents (3, 4). These pre-steady-state currents were central in formulating a detailed quantitative nonrapid equilibrium six-state kinetic model of Na^+/glucose transport (5). This model (see Fig. 4*A*) assumes a valence of −2 for the transporter and that translocation of the empty transporter and Na^+ binding are both voltage dependent. The kinetics are ordered, with two Na^+ ions binding prior to the binding of sugar. The fully loaded transporter then reorients in the membrane and releases sugar and Na^+ to the cytoplasm, and the cycle is completed by the reorientation of the empty sugar and Na^+ binding sites back to the external face of the membrane. According to this model, pre-steady-state currents observed after a voltage step are due to the charge transfer involved in the dissociation of external Na^+ and the reorientation of the unloaded SGLT1 protein (C, for carrier) in the membrane: $[CNa_2]' \rightleftarrows [C]' \rightleftarrows [C]''$ (Fig. 4*A*).

Here we have isolated the SGLT1 pre-steady-state currents, using a fast two-electrode voltage clamp, and have determined their kinetics as a function of voltage and Na^+ and sugar concentrations. The results enable us to estimate the number of transporters in the membrane, the apparent valence of the voltage sensor, and rates for the voltage-dependent steps in the transport reaction cycle (see Fig. 4*A*). Analysis of pre-steady-state currents, therefore, represents a powerful experimental approach to understanding the mechanisms for the transport of solutes into cells by cotransporters.

MATERIALS AND METHODS

Human SGLT1 (hSGLT1) (6) was expressed in *Xenopus laevis* oocytes, and experiments were performed on oocytes 5–14 days after injection of complementary RNA (cRNA). Membrane currents were measured by using a two-electrode voltage clamp (3, 4), but in this series of experiments we used a faster clamp amplifier (settling time of 0.5 ms for a 100-mV step). The interior of the oocyte was maintained at virtual earth potential (7). Microelectrodes with resistances of 1–2 and 0.5–1 MΩ were used for the voltage recording and injection of current, respectively. Step changes in membrane potential (V_m) from the holding potential (V_h) were applied and currents were averaged from 15 sweeps. The currents were low-pass filtered at 5 kHz by a nine-pole Bessel filter, digitized at 26 μs per point, and displayed at 52 μs per point.

Oocyte membrane capacitance (C_m) was determined from the slope of the Q versus voltage relation for 10- to 20-mV hyperpolarizing pulses from V_h (−100 mV). In control H_2O-injected oocytes current relaxations showed a single time constant ($\tau \approx 0.5$ ms; cf. Fig. 1*C*), and the integral of the capacitive transients was a linear function of the voltage step ($V_t - V_h$). The capacitance ranged between 175 and 250 nF per oocyte, comparable to that reported previously (8). In cRNA-injected oocytes, the total current relaxation showed two components for depolarizing pulses (see also figure 1*A* of ref. 3 and figure 7*A* of ref. 4): the capacitive current ($\tau \approx 0.5$ ms) and the transient currents due to hSGLT1 ($\tau \approx$ 2–10 ms). The integral of the total current relaxation was a nonlinear function of voltage. To isolate hSGLT1 transient currents three methods were used: (*i*) the standard P/4 protocol (9) with a subpulse holding potential of −100 mV; (*ii*) a phlorizin-block method in which currents were measured in the presence and absence of phlorizin (see figure 7*B* of ref. 4)

The publication costs of this article were defrayed in part by page charge payment. This article must therefore be hereby marked "*advertisement*" in accordance with 18 U.S.C. §1734 solely to indicate this fact.

Abbreviations: SGLT1, Na^+/glucose cotransporter; hSGLT1, human SGLT1; cRNA, complementary RNA; αMeGlc, α-methyl D-glucopyranoside.

(phlorizin is a specific inhibitor of Na^+/glucose cotransport); and (*iii*) a fitted method, in which the total current $I(t)$ was fitted to $I(t) = I_1e^{-t/\tau_1} + I_2e^{-t/\tau_2} + I_{ss}$ (figure 8 of ref. 4), where I_1 is the capacitance current with time constant τ_1, t is time, I_2 is the SGLT1 transient current with time constant τ_2, and I_{ss} is the steady-state current. Transient currents and the total charge Q (integral of the transient current) due to hSGLT1 were similar for all methods (see Fig. 1*D*). However, we routinely used the fitted method, as in the presence of sugar the P/4 method could not be applied because the background currents (due to the steady-state inward Na^+ currents via the cotransporter) were nonlinear (see figure 2*A* of ref. 3, figure 2 of ref. 4, or figure 2*A* of ref. 10) and current records obtained by using the fitted method were less noisy than the records obtained by using the phlorizin-block method. The steady-state sugar-dependent inward Na^+ currents (cf. Fig. 2 *A* and *D*) were obtained as the difference in steady-state current measured in the presence and in the absence of sugar (figure 1*D* of ref. 3 or figure 2*B* of ref. 4). In general, each of the results described was for experiments carried out in one oocyte, but all were performed at least three times on oocytes from different donors.

Oocytes were bathed in a buffer containing (mM): 100 NaCl, 2 KCl, 1 $CaCl_2$, 1 $MgCl_2$, and 10 Hepes (pH 7.4). The composition of the bathing solution was varied by replacing NaCl (100–0 mM) with choline chloride, adding sugar (α-methyl D-glucopyranoside, αMeGlc) and/or phlorizin (see text and figure legends).

RESULTS

Fig. 1*A* shows current records in a cRNA-injected oocyte bathed in NaCl buffer without sugar. Stepping the membrane potential from the holding potential (V_h = −100 mV) to the test potential (V_t = −150 to +50 mV) induced current transients (time constant $\tau \approx$ 2–10 ms) distinct from capacitive current spikes ($\tau \approx$ 0.5 ms). Transient currents were never observed in control H_2O-injected oocytes (see figure 1*A* of ref. 4). Subtraction of capacitive and steady-state currents yields the transient current due to hSGLT1 (Fig. 1*B*). The relaxation time constants τ of the transients were voltage dependent, ranging from 8 ms at V_t = −50 mV to 2 ms at V_t = +50 mV (Fig. 1*C*). In the off response, τ (9 ± 0.5 ms, n = 7) was independent of V_t (□ in Fig. 1*C*). The time constant due to the oocyte membrane capacitance (◆ in Fig. 1*C*) was relatively insensitive to voltage. Charge transfer Q for the on response is similar when the P/4 and the fitted methods are used (Fig. 1*D*). Q for the on and off responses is shown in Fig. 1*E*. At V_h = −100 mV, Q was equal for the on and off responses and saturated with V_t. The data are described by the Boltzmann equation (see the legend for Fig. 1*E*) with Q_{max} = 21 nC, $V_{0.5}$ = −39 mV, and z = 1.0. Fig. 1*E* also shows that Q_{max}, $V_{0.5}$, and z were independent of V_h. z provides a measure of the effective valence of the movable charge. Q_{max} varied from oocyte to oocyte (up to 60 nC), but for each oocyte Q_{max} obtained in the absence of sugar was proportional to I^s_{max}, the steady-state Na^+ current induced by saturating sugar concentrations at V_t = −150 mV, which has been shown to provide an index of the level of SGLT1 expression (3, 4, 10). The pooled data plot (from eight oocytes) of I^s_{max} vs. Q_{max} yields a slope of 57 ± 5 s^{-1}. If Q_{max} represents the number of transporters in the membrane, this slope is an estimate of the turnover of the transporter (see Fig. 4*A*).

The effects of sugar on Q_{max} and on steady-state sugar-induced inward Na^+ current are shown in Fig. 2. Transient and steady-state sugar-induced currents were measured in the presence of 0–20 mM sugar at V_t = +30 and −130 mV with a V_h of −50 mV. Increasing sugar concentration reduced transient currents (this is more apparent in off response

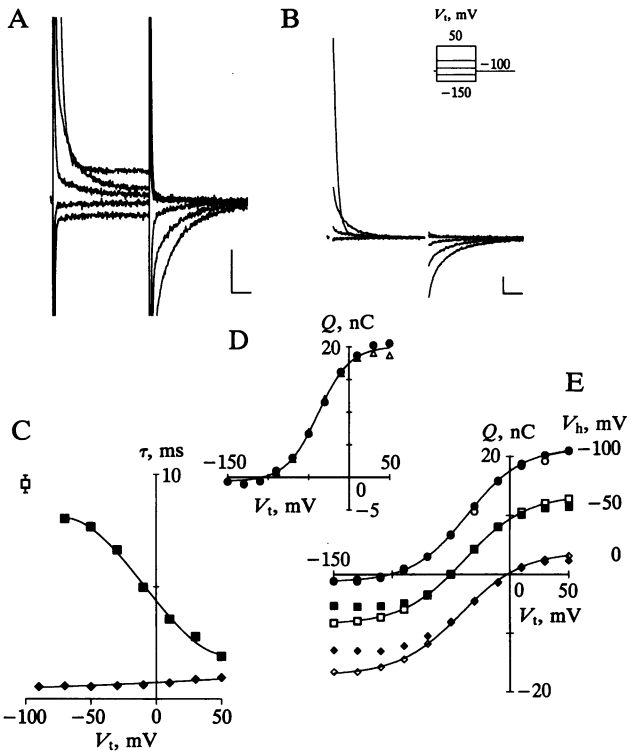

FIG. 1. Charge translocation in an oocyte injected with hSGLT1 cRNA. (*A*) Membrane current records. Membrane potential (V_m) was stepped from V_h of −100 mV to V_t of +50, −30, −70, −110, and −150 mV. Current relaxation showed two components: the capacitive current ($\tau \approx$ 500 μs, see ◆ in *C*) and the transient currents ($\tau \approx$ 2 ms at V_t = +50 mV; see ■ in Fig. 1*C*). The crossing of the current records at V_t = +50 and −30 mV was due to saturation of Q and decrease in time constant τ with depolarization (see *C* and *D*). Vertical bar, 0.5 μA; horizontal bar, 10 ms. (*B*) Carrier-mediated displacement or transient currents. These were obtained from the total currents in *A* by subtraction of the capacitive and steady-state currents, using the fitted method. They are displayed 1.6 ms after the voltage step. At this time the ratio of the transient to capacitive currents was greater than 4 at V_t = +50 mV. Vertical bar, 0.5 μA; horizontal bar, 10 ms. (*C*) Kinetics of transient current relaxation. The relaxation on (■) and off (□) currents were described by a single time constant (τ) between 1.6 ms and the steady state. ◆ is the time constant due to the oocyte membrane capacitance. The smooth curves were drawn by eye. (*D*) Charge–voltage relationship obtained by using the fitted method (●) and the P/4 protocol (△). The smooth curve was drawn by eye. (*E*) Charge transfer. Q was obtained from integration of the transient currents during the on (filled symbols) and off (open symbols) responses for V_h = −100 (○), −50 (□), and 0 (◇) mV. Q was the same for the on and off responses (for all depolarizing and for hyperpolarizing potentials ≤40 mV from V_h). At each V_h the data were fitted (smooth curves) to the Boltzmann equation, $(Q - Q_{hyp})/Q_{max} = 1/[1 + \exp(z(V_t - V_{0.5})F/RT)]$, in which $Q_{max} = Q_{dep} - Q_{hyp}$, Q_{dep} and Q_{hyp} being Q at depolarizing and hyperpolarizing limits, and varied with V_h. F, Faraday's constant; R, the gas constant; T, absolute temperature; $V_{0.5}$, the potential for 50% charge transfer; and z, the apparent valence of the movable charge. All data were from a single *Xenopus* oocyte injected with cRNA coding for hSGLT1 (6). The oocyte was bathed in a 100 mM NaCl solution without sugar at 25°C.

records, Fig. 2*B*) and reduced Q_{max} (Fig. 2*C*). The reduction was hyperbolic, with 50% Q_{max} at 1 mM αMeGlc, close to the apparent $K^{\alpha MeGlc}_{0.5}$ (0.8 mM) for the steady-state sugar-induced current measured in this oocyte. The decrease in Q_{max} was directly proportional to the increase in the steady-state inward Na^+ current induced by sugar (Fig. 2*D*), with a slope of 84 ± 7 s^{-1}. Reductions of Q_{max} were also obtained with 10–100 μM phlorizin in the absence of sugar.

hSGLT1 transient currents were measured as a function of external Na^+ concentration, $[Na]_o$. As $[Na]_o$ was reduced

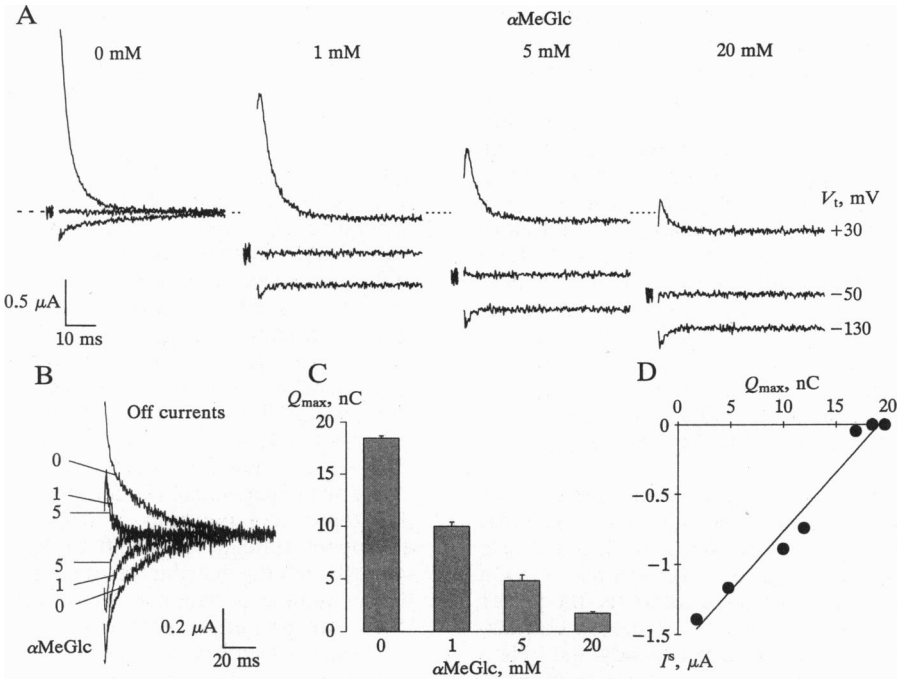

FIG. 2. Effect of sugar on transient and steady-state currents. (*A*) Transient and steady-state current records in the presence of 0–20 mM αMeGlc in the Na buffer (100 mM Na^+). V_h was −50 mV and the membrane was stepped to +30 and −130 mV. The current records were obtained by adding the transient currents isolated by using the fitted method to the steady-state sugar-induced inward Na^+ current (I^s), which was obtained as the difference in steady-state current measured in the presence and in the absence of sugar. Similar records were obtained by subtracting the current records measured in the presence of saturating phlorizin from the current records measured in the presence of 0–20 mM sugar. The broken line indicates zero current. (*B*) Transient currents for the off response when V_t (+30 mV inward currents and −130 mV outward currents) was returned to V_h = −50 mV in the presence of 0–20 mM αMeGlc. The off currents were inward and outward, respectively, for V_t = +30 and −130 mV. For comparison of the off currents at different sugar concentrations, the steady-state currents have been removed. (*C*) Q_{max} as a function of αMeGlc. Q_{max} was measured at each sugar concentration as described for Fig. 1*E*. (*D*) Plot of I^s vs. Q_{max}. I^s was measured at −150 mV, where it was independent of V_t (3, 4, 10). The line was a linear regression, and the slope was 84 ± 7 s^{-1}. This experiment was carried out on a hSGLT1 cRNA-injected oocyte as in Fig. 1, at 20°C. C_m was 215 nF. $K_{0.5}$ and I^s_{max} for the sugar-induced steady-state current were 0.8 mM and 1.5 μA at V_t = −150 mV.

from 100 to 10 mM there was a 40% decrease in Q_{max}, no effect on z, and a shift in $V_{0.5}$ from −39 to −70 mV (Fig. 3*A*). Furthermore, as $[Na]_o$ was decreased there was a reduction in the current relaxation time constant τ, especially at more negative values of V_t (Fig. 3*B*); lowering $[Na]_o$ therefore reduced the voltage dependence of τ. Charge transfer was also observed on oocytes bathed in the nominal absence of external Na^+, but we were unable to determine Q_{max} because Q did not saturate at the largest hyperpolarizing potential applied (−190 mV).

Finally, hSGLT1 transient currents and charge transfer were measured as a function of temperature. Between 20 and 30°C there was no significant effect on Q_{max} (Fig. 3*C*), but τ decreased as the temperature increased (Fig. 3*D*), especially at negative values of V_t (Q_{10}, the factor for a 10°C temperature change, was 2.5 at −50 mV). Thus lowering $[Na]_o$ or increasing temperature produced a similar decrease in the time constant τ.

DISCUSSION

Progress in our understanding of the coupling between substrate and ion transport by cotransport proteins has been

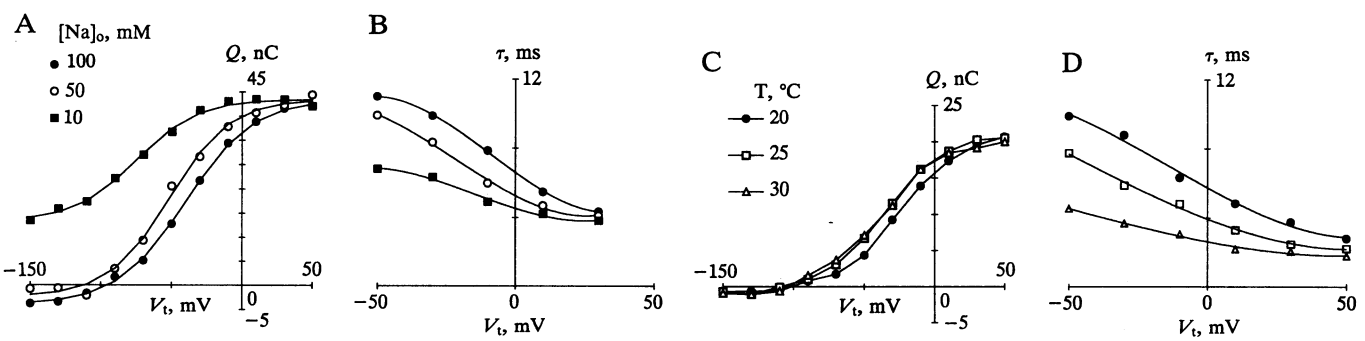

FIG. 3. Effect of external Na^+ concentration, $[Na]_o$, on transient currents. The smooth curves were drawn by eye. (*A*) Q as a function of $[Na]_o$. For comparison, the curves of Q vs. V_t for 10 and 50 mM Na_o have been shifted vertically so that Q at the extreme depolarizing potentials for $[Na]_o$ of 100, 50, and 10 mM is the same. (*B*) τ as a function of $[Na]_o$. The experiment in *A* and *B* was carried out on a hSGLT1 cRNA-injected oocyte as in Fig. 1. The Na^+ in the bathing solution was varied between 100 and 10 mM by replacing NaCl with choline chloride. V_h was −100 mV and the temperature was 20°C. C_m was 243 nF. (*C*) Charge–voltage relations as a function of temperature. The temperature of the bath was varied between 20 and 30°C and Q and τ were determined as in Fig. 1. C_m was 215 nF; V_h was −100 mV, and $[Na]_o$ was 100 mM. (*D*) Effect of temperature on τ. Bath temperature was varied between 20 and 30°C. The experiment was performed on the same oocyte as *C*.

impeded by a lack of methods to study these rare integral membrane proteins. This has been alleviated to some extent by the cloning and overexpression of cotransporters in oocytes. Nevertheless, cotransporter kinetics have generally been studied by steady-state methods. It has been necessary to make assumptions about the number of transporters in the membrane, the order of substrate binding, the rate-limiting steps (rapid equilibrium vs. nonrapid equilibrium models), and the voltage-dependent steps. For example, in the nonrapid equilibrium, ordered model illustrated in Fig. 4, there are 14 terms, and with steady-state fluxes alone it is impossible to extract a numerical fit for these 14 terms. However, in voltage-clamp experiments we recently observed pre-steady-state SGLT1 currents, and the general characteristics of these currents impose limits on at least 4 of these rate constants. This has enabled us to obtain one set of rate constants that quantitatively accounts for Na^+/glucose cotransport (5).

The power of pre-steady-state (relaxation) methods to examine chemical reaction kinetics has long been recognized, and in membrane biology pre-steady-state electrical methods have been used to much advantage to study the kinetics of ion channels (11, 12). In this study we have combined the power of the overexpression of the cloned Na^+/glucose cotransporter in oocytes with now classical pre-steady-state electrophysiological methods to examine the relaxation steps of the cotransporter. Pre-steady-state SGLT1 currents were measured as a function of voltage and Na^+, sugar, and phlorizin concentrations, and the kinetics of the SGLT1 charge transfer have enabled us to test our kinetic model. Basically by controlling the experimental conditions we are able to study two partial reactions of the kinetic scheme.

We conclude that transient currents observed in oocytes expressing SGLT1 are due to charge transfer by SGLT1. This is supported by the following observations: (*i*) these transient currents are seen only in oocytes injected with SGLT1 cRNA (see figure 1 of ref. 4); (*ii*) charge movements (Q) measured during the onset and off of the voltage pulse are equal and opposite (Fig. 1*E*); (*iii*) Q saturates with either hyperpolarization or depolarization (Fig. 1*E*); (*iv*) reversal of Q occurs at the holding potential V_h (Fig. 1*E*); and (*v*) Q_{max} is directly proportional to the number of functional hSGLT1 proteins expressed. Q_{max} values of ≈25 nC per oocyte correspond to $\approx 10^{11}$ carriers per oocyte or $\approx 10^4/\mu m^2$. This is comparable with the density of *Halobacterium* rhodopsin, sarcoplasmic reticulum Ca-ATPase, and *Torpedo* acetylcholine receptors (13). Furthermore, Q_{max} is (*vi*) independent of holding potential (Fig. 1*E*); (*vii*) apparently eliminated by saturating sugar concentrations (Fig. 2 *A* and *D*) and phlorizin (unpublished data; figure 7 of ref. 4); and (*viii*) independent of temperature (Fig. 3*C*). The rate of charge transfer is, however, temperature dependent, with a Q_{10} of 2.5 for τ (Fig. 3*D*).

The sugar-dependent reduction in Q_{max} (Fig. 2*A*) indicates that there is a partition of hSGLT1 into a non-voltage-dependent state(s). The shift in $V_{0.5}$ with $[Na]_o$ (Fig. 3*A*) suggests that the distribution of conformations of hSGLT1 in the membrane is dependent on $[Na]_o$—i.e., the higher the $[Na]_o$, the greater the percentage of SGLT1 proteins facing the external membrane surface.

What is the origin of the SGLT1 charge movement? This can be discussed in terms of the six-state ordered kinetic model (Fig. 4*A*) proposed for the Na^+/glucose cotransporter (5). The model assumes that (*i*) on both membrane surfaces, the transporter can be empty (C), loaded with Na^+ (CNa_2), or fully loaded with Na^+ and sugar ($SCNa_2$); (*ii*) the transporter has a valence of −2; (*iii*) the transporter binds to two Na^+ ions to form an electroneutral CNa_2 before binding sugar; (*iv*) C, CNa_2, and $SCNa_2$ can cross the membrane; and

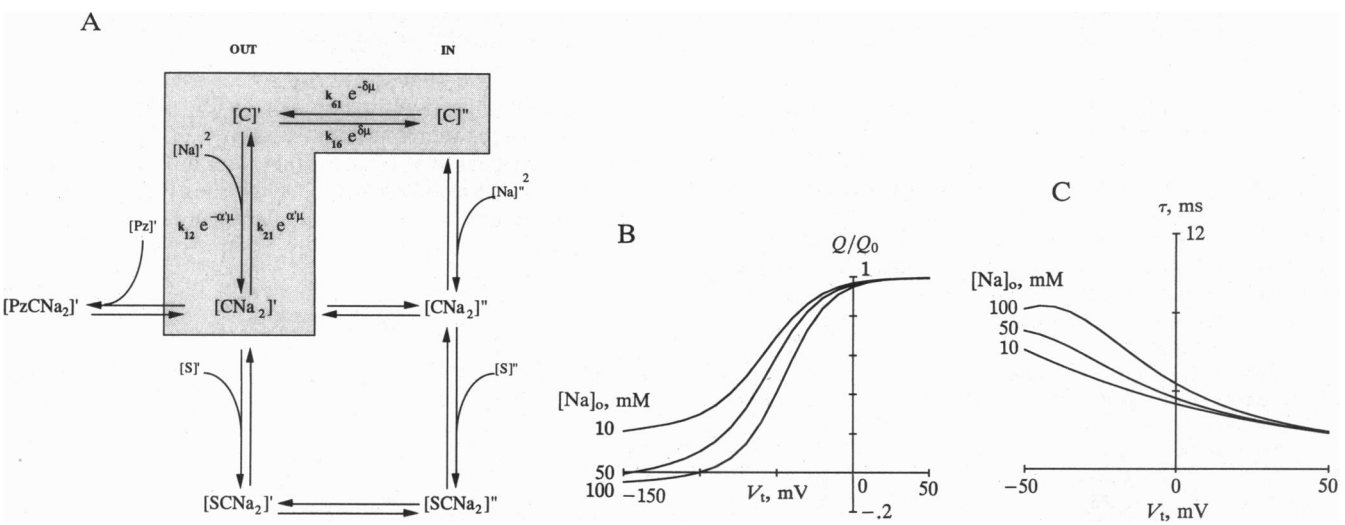

FIG. 4. Kinetic model for Na^+/glucose cotransport. (*A*) A six-state kinetic model of hSGLT1 expressed in oocytes (5). Two Na^+ ions bind to the carrier (valence, −2) before the binding of sugar. The empty carrier C, the Na^+-loaded carrier CNa_2, and the sugar-loaded carrier $SCNa_2$ can cross the membrane. Membrane voltage affects Na^+ binding with the carrier and translocation of the empty carrier across the membrane. Since transient charge transfers are eliminated by transported sugars (Fig. 2) and phlorizin (not shown), we conclude that only three (shaded region) of the six states effectively participate in charge transfer, [C]', [CNa_2]', and [C]". For simplicity, we do not consider [CNa_2]", the Na^+ form of the protein facing the cytoplasm, since the intracellular Na^+ is low (≈10 mM) relative to the extracellular concentration. Transitions between [CNa_2]' and [CNa_2]" are negligibly small (4, 10). The three-states reaction scheme is described by four rate constants, k_{12}, k_{21}, k_{16}, and k_{61}, and two constants, α' and δ, representing the fraction of the electrical field across the membrane influencing Na^+ binding and translocation of the empty carrier. We also assumed that there is no voltage dependence for internal Na^+ binding—i.e., $\alpha'' = 0$. Thus $\alpha' + \delta = 1$ (5). Phlorizin (Pz) binds to the Na^+-loaded transporter [CNa_2]' to form the inactive complex [$PzCNa_2$]'. (*B* and *C*) Model prediction of hSGLT1 charge transfer. The curves are the predictions based on simulation of the three-state model (shaded region in *A*) with $\alpha' = 0.3$, $\delta = 0.7$, $k_{16} = 600\ s^{-1}$, $k_{61} = 25\ s^{-1}$, $k_{12} = 14{,}000\ s^{-1}\cdot M^{-2}$, $k_{21} = 300\ s^{-1}$, and $[Na]_o$ = 100, 50, and 10 mM. The simulation was performed with $V_h = -100$ mV. (*B*) Q as a function of voltage and $[Na]_o$. For comparison, all three curves have been normalized by Q_o, the maximal charge at large depolarizing potentials at $[Na]_o$ = 100 mM, and the curves for $[Na]_o$ = 50 and 10 mM have been shifted to coincide with the $[Na]_o$ = 100 mM curve at large depolarizing potentials. (*C*) τ as a function of voltage and $[Na]_o$. The model also predicts a second, faster, time constant which is beyond the resolution of the current technique. Q was obtained by numerical integration, and τ by eigenvalue analysis, of the pre-steady-state current equation (see equations A44–A50 of ref. 5).

(v) membrane voltage affects Na^+ binding to the transporter and translocation of the empty transporter across the membrane. With these assumptions, estimates were obtained for all the rates of partial reaction steps (5). The model can account qualitatively and quantitatively for the kinetics of the Na^+/glucose cotransporter expressed in *Xenopus* oocytes (5). The model also predicts that in the absence of sugar, pre-steady-state currents or charge transfer originate from voltage-dependent Na^+ binding at the external side of the cotransporter in the membrane and voltage-dependent conformational changes of the empty carrier. At 100 mM Na_o and V_h −50 mV, the carrier is in state $[CNa_2]'$ poised to bind external sugar or phlorizin (Fig. 4*A*). Rapid depolarization of the membrane to +50 mV results in Na^+ dissociation to form $[C]'$, and the negatively charged protein reorients in the field. In summary, the model predicts that charge movement is due to Na^+ binding from the transporter and reorientation of the transporter in the membrane.

Our observations on hSGLT1 pre-steady-state currents are consistent with the predictions of this model. In our experiments, Q_{max} decreased with decreasing $[Na]_o$, and indeed charge movement was also observed in Na^+-free conditions. Thus both Na^+ binding and the reorientation of the empty carrier contribute to charge movement. Moreover, according to the model, sugar eliminates the charge translocation by partitioning the carrier to the states $[CNa_2S]'$ and $[CNa_2]''$, thereby effectively decreasing Q by reducing the concentration of $[CNa_2]'$ (5). This partitioning of the carrier states by sugar is supported by the results of Fig. 2*D*. In addition to sugar, we have found that phlorizin also eliminates charge transfer, implying that sodium is unable to dissociate from the carrier in the presence of the blocker.

We have simulated the kinetics of the transient currents of hSGLT1 in the absence of sugar, assuming that charge transfer is due to interconversion of the three state $[CNa_2]' \rightleftarrows [C]' \rightleftarrows [C]''$ (shaded region, Fig. 4*A*) with $\alpha' = 0.3$, $\delta = 0.7$, $k_{21} = 300\ s^{-1}$, $k_{12} = 14{,}000\ s^{-1}\cdot M^{-2}$, $k_{16} = 600\ s^{-1}$, and $k_{61} = 25\ s^{-1}$. Results of the simulation at 100, 50, and 10 mM $[Na]_o$ are shown for the charge–voltage relationship (Fig. 4*B*) and for the voltage dependence of τ (Fig. 4*C*). The model accounts qualitatively for the dependence of charge transfer Q and the time constant τ on membrane voltage and $[Na]_o$ (Fig. 3*B*) as well as the dependence of Q_{max} on $[Na]_o$ and the shifting of $V_{0.5}$ to more negative values with decreasing $[Na]_o$ (Fig. 3*A*). According to the simulation, both Na^+ binding and the reorientation of the carrier in the membrane contribute to charge movement, with the latter being the major (70%) charge translocation step. This analysis suggests that for the human cotransporter the rate-limiting step upon depolarization of the membrane is the dissociation of Na^+ from the protein (k_{21}). In our experiments, only one time constant τ was observed. However, the model predicts a second, faster time constant and may be observed with a faster voltage clamp such as that achieved with the split oocyte technique (12, 14).

These kinetic parameters determined from charge transfer measurements alone are in close agreement with those previously determined to account for the global electrical properties of the rabbit cotransporter (5); i.e., $\alpha' = 0.3$, $\delta = 0.7$, $k_{21} = 500\ s^{-1}$, $k_{12} = 80{,}000\ s^{-1}\cdot M^{-2}$, $k_{16} = 35\ s^{-1}$, and $k_{61} = 5\ s^{-1}$. The most obvious difference is in $k_{16}/k_{21} > 1$ (human) vs. < 0.1 (rabbit). The two sets of rate constants can account for the difference between the voltage dependence of τ in the two species: τ increases with depolarization for rabbit SGLT1 (see figure 9*A* of ref. 4), while it decreases with depolarization for hSGLT1 (Fig. 1*C*). The difference in the primary amino acid sequences between the rabbit and human cotransporters (85% identity, 94% similarity, see ref. 2) must account for this kinetic difference.

In conclusion, we have demonstrated that charge movements can be recorded for the Na^+/glucose cotransporter and that these pre-steady-state currents provide estimates of both the number of functional carriers in the membrane and the rates of steps (k_{16}, k_{61}, k_{12}, and k_{21}) in the transport cycle. Charge translocations have also been recorded for the cardiac Na^+/K^+ pump (15) and for the cloned Na^+/myoinositol (16, 17) and $Na^+/Cl^-/\gamma$-aminobutyrate cotransporter expressed in oocytes (18). This indicates that transient currents may be a general property of membrane pumps and transporters. Combining charge transfer measurements with genetic engineering of cloned transport proteins can therefore be expected to provide a powerful tool for studying transport mechanisms.

We thank F. Bezanilla and E. Perozo for design of the amplifier; K. Hager for providing and assisting with the oocytes; and F. Bezanilla and B. Hirayama for their helpful comments and review of the manuscript. This work was supported by National Institutes of Health Grants DK19567 and NS25554.

1. Griffith, J. K., Baker, M. E., Rouch, D. A., Page, M. G. P., Skurray, R. A., Paulsen, I. T., Chater, K. F., Baldwin, S. A. & Henderson, J. F. (1992) *Curr. Opin. Cell Biol.* **4**, 684–695.
2. Wright, E. M., Hager, K. & Turk, T. (1992) *Curr. Opin. Cell Biol.* **4**, 696–702.
3. Birnir, B., Loo, D. D. F. & Wright, E. M. (1991) *Pflügers Arch.* **418**, 79–85.
4. Parent, L., Supplisson, S., Loo, D. D. F. & Wright, E. M. (1992) *J. Membr. Biol.* **125**, 49–62.
5. Parent, L., Supplisson, S., Loo, D. D. F. & Wright, E. M. (1992) *J. Membr. Biol.* **125**, 63–79.
6. Hediger, M. A., Turk, E. & Wright, E. M. (1989) *Proc. Natl. Acad. Sci. USA* **86**, 5748–5752.
7. Vaughan, P. C., McLarnon, J. G. & Loo, D. D. F. (1980) *Can. J. Physiol. Pharmacol.* **58**, 999–1010.
8. Kado, R. T. (1983) in *Physiology of Excitable Cells: Neurology and Neurology*, eds. Grinnell, A. D. & Moody, W. J. (Liss, New York), Vol. 5, p. 247.
9. Bezanilla, F. & Armstrong, C. M. (1977) *J. Gen. Physiol.* **70**, 549–566.
10. Umbach, J. A., Coady, M. J. & Wright, E. M. (1990) *Biophys. J.* **57**, 1217–1224.
11. Armstrong, C. M. & Bezanilla, F. (1973) *Nature (London)* **242**, 459–461.
12. Bezanilla, F., Perozo, E., Papazian, D. M. & Stefani, E. (1991) *Science* **254**, 679–683.
13. Hille, B. (1992) *Ionic Channels of Excitable Membranes* (Sinauer, Sunderland, MA), 2nd Ed.
14. Taglialatela, M., Toro, L. & Stefani, E. (1992) *Biophys. J.* **61**, 78–82.
15. Nakao, M. & Gadsby, D. C. (1986) *Nature (London)* **323**, 628–630.
16. Kwon, H. M., Yamauchi, A., Uchida, S., Preston, A. S., Garcia-Perez, A., Burg, M. B. & Handler, J. S. (1992) *J. Biol. Chem.* **267**, 6297–6301.
17. Hazama, A., Hager, K., Kwon, H. M. & Loo, D. D. F. (1993) *FASEB J.* **7**, A575 (abstr.).
18. Mager, S., Naeve, J., Quick, M., Labarca, C., Davidson, N. & Lester, H. A. (1993) *Neuron* **10**, 177–188.